Characterization of the Saffron Derivative Crocetin as an Inhibitor of Human Lactate Dehydrogenase 5 in the Antiglycolytic Approach against Cancer

Carlotta ***Granchi***,[a] *Serena* ***Fortunato*** [a] *Serena* ***Meini***,[a] *Flavio* ***Rizzolio***,[c] *Isabella* ***Caligiuri***,[d] *Tiziano* ***Tuccinardi***,[a,e] *Hyang Yeon* ***Lee***,[b] *Paul J.* ***Hergenrother***,[b] *Filippo* ***Minutolo***,[a,e,*]

[a] Dipartimento di Farmacia, Università di Pisa, Via Bonanno 6 and 33, 56126 Pisa, Italy.

[b] Department of Chemistry, University of Illinois at Urbana-Champaign, 600 S. Mathews, Urbana, Illinois 61801, USA.

[c] Dipartimento di Scienze Molecolari e Nanosistemi, Università Ca'Foscari, Venezia, Italy.

[d] Division of Experimental and Clinical Pharmacology, Department of Molecular Biology and Translational Research, National Cancer Institute and Center for Molecular Biomedicine, Aviano (PN), Italy

[e] Centro Interdipartimentale di Ricerca "Nutraceutica e Alimentazione per la Salute", Università di Pisa, Via del Borghetto 80, 56124 Pisa, Italy.

AUTHOR INFORMATION

Corresponding Author

*Corresponding author phone: +39 050-2219557; fax +39 050-2210680; e-mail: filippo.minutolo@unipi.it

Title running header: Crocetin inhibits LDH in glycolytic cancer cells

ABSTRACT

Inhibition of lactate dehydrogenase (LDH) represents an innovative approach to tackle cancer because this peculiar glycolytic metabolism is characteristic of most invasive tumor cells. An investigation into the biological properties of saffron extracts led to the discover of their LDH-inhibition properties. In particular, the most important saffron components, crocetin, was found to inhibit LDH (IC_{50} = 54.9 ± 4.7 μM). This carotenoid was independently produced by chemical synthesis, and its LDH-inhibition properties manifested via its antiproliferative activity against two glycolytic cancer cell lines (A549 and HeLa, IC_{50} = 114.0 ± 8.0 and 113.0 ± 11.1 μM, respectively). The results described in this article suggest that saffron may be a helpful alimentary component in the prevention of cancer that potentially contributes to the efficacy of approved cancer therapies.

KEYWORDS

- Saffron;
- cancer;
- crocetin;
- lactate dehydrogenase;
- glycolysis

INTRODUCTION

Inhibition of lactate dehydrogenase (LDH) as a potential anticancer strategy is rationalized via Otto Warburg's observation that cancer cells rapidly internalize and consume glucose to survive, which in turn produces large amounts of lactate.[1] In the last decade, a great interest was directed towards the discovery of antiglycolytic agents capable of interfering with the glycolytic metabolism of cancer cells.[2,3] In this context, the human homotetrameric isoform 5 of lactate dehydrogenase (*h*LDH-5), composed of four A subunits, is considered a strategic target to selectively disrupt the metabolism of cancer cells. Moreover, *h*LDH-5 is overexpressed in many types of tumours. *h*LDH-5 catalyzes the last step of glycolysis - the reversible reduction of pyruvate to lactate via the simultaneous oxidation of NADH to NAD^+. Considering the essential role of this enzyme in the regeneration of NAD^+ and continuation of glycolysis, we hypothesized its inhibition should lead to cancer cell death by starvation. Individuals that lack of *h*LDH-5 experience myoglobinuria after intense anaerobic exercise yet are healthy under ordinary circumstances. Therefore, we hypothesize that the inhibition of *h*LDH-5 is a potentially safe approach to treating cancer that will avoid the deleterious side-effects associated with traditional chemotherapy.[4] Previously, *h*LDH-5 was silenced with *si*RNA, resulting in an evident decrease in cancer cell proliferation and migration.[5] These results laid the groundwork for the development and the synthesis of many small molecules as *h*LDH-5 inhibitors and several proved to be potent inhibitors both *in vitro* and *in vivo*.[6] However, the search for new potent inhibitors remains a challenging goal, since the cavity of the enzyme comprises both a cofactor (NADH)- and a substrate (pyruvate)-binding pocket. The substrate-binding site is very narrow, polar, and possesses many positively charged residues, whereas, the cofactor binding region is quite extended since NADH binds to the enzyme with the nicotinamide and adenosine portions at opposite ends of this site.

Several natural products have been identified as *h*LDH-5 inhibitors. One of the first examples is represented by the natural derivative gossypol (Figure 1), which is extracted from the cotton seeds of the *Gossypium* species. Gossypol was initially studied as an antimalarial agent, due to its inhibitory

activity of the *Plasmodium falciparum* isoform of LDH (*pf*LDH). However, this compound proved to be a non-selective competitive inhibitor of LDH relative to NADH through its inhibition of the human LDH isoforms. Additionally, the high toxicity of gossypol (including cardiac arrhythmias, renal failure, muscle weakness and even paralysis) hampered its further development as an anticancer agent.[7] Later, the flavonoid epigallocatechin[8] (Figure 1) and the fungal metabolite panepoxydone[9] (Figure 1) exerted an indirect inhibitory effect on *h*LDH-5 by reducing its expression in cancer cells. Conversely, the α,β-unsaturated aldehyde 4-hydroxy-2-nonenal (Figure 1), which naturally forms upon oxidation of unsaturated fatty acids, covalently binds the enzyme and blocks its activity.[10] The recently identified *h*LDH-5 inhibitor penta-1,2,3,4,6-*O*-galloyl-β-D-glucose (Figure 1), a component of *Rhus Chinensis* gallnut extract, directly inhibits the enzyme via competitive displacement of the cofactor NADH.[11] Galloflavin (Figure 1), a compound formed via autooxidation of the natural compound gallic acid, was identified by virtual screening of compounds from National Cancer Institute dataset and proved to inhibit both *h*LDH-5 and *h*LDH-1 with K_i values in the micromolar range and retard cancer cell growth.[12] Luteolin 7-*O*-β-D-glucopyranoside (Figure 1) isolated from *Phlomis kurdica*, inhibits *h*LDH-5 with an IC_{50} value in the micromolar range. It was shown to be competitive with NADH; a conclusion supported by modelling studies.[13] Moreover, a high-throughput screening of medicinal plants identified some natural extracts, such as Chinese Gallnut (*Melaphis chinensis gallnut*), Bladderwrack (*Fucus vesiculosus*), Kelp (*Laminaria Japonica*) and Babul (*Acacia Arabica*) that showed *h*LDH-5 IC_{50} values lower than 0.001 mg/ml, although the individual chemical constituents responsible for the activity were not isolated.[14]

Given that a growing number of natural products have demonstrated the ability to directly and indirectly *h*LDH-5, we screened a large panel of natural products that are mostly found in alimentary sources for the purpose of identifying new natural products as food-derived *h*LDH-5 inhibitors. As such, we sought to identify a possible nutraceutical strategy to produce safe antiglycolytic effects that might prove to be helpful for the prevention and treatment of cancer. In particular, we were intrigued by the well-known anticancer properties of saffron, which is one of the most expensive spices in the

world and widely known for its deep yellow colour and exquisite taste. Saffron has long been used as a medicinal herb to treat several diseases in traditional medicine, and it has found many therapeutic applications resulting from the plethora of pharmacological properties of its components.[15-18] Saffron consists of the dried red stigmas of *Crocus sativus Linnaeus* flowers, and its main components can be grouped in three principle classes: 1) crocins: water-soluble coloured compounds that are glycosides of the carotenoid crocetin with various sugar ester moieties; 2) picrocrocin: a monoterpene glycoside that is the main substances responsible for saffron's bitter taste; 3) safranal: the volatile oil responsible for the characteristic saffron aroma (Figure 2).[19,20]

In order to investigate if any of the saffron components possess anti-LDH activity and contribute to its reported anticancer activity,[16] we started our study by analysing the effects of this spice on the isolated enzyme. Furthermore, among the main components of saffron, it is widely documented that both crocin, the crocetin digentiobiose ester, which represents the most important glycoside carotenoid,[21-24] and also the carotenoid aglycon itself, crocetin, exert anticancer and chemopreventive effects on several types of cancer cells, and some *in vivo* animal models.[25-29] It is important to note that the average content of crocin, which behaves as a direct bioprecursor of crocetin when administered in vivo,[30] is about 40 mg/g of stigmas, depending on the geographical location of the saffron source.[31] Furthermore, the bioavailability of crocetin after oral administration to human volunteers proved to be highly satisfactory. It was rapidly absorbed and reached maximal plasma concentration of up to 1 uM after 4-5 hours even at the relatively low dose of 22.5 mg.[32]

Interestingly, Kim *et al.* recently reported the effects of crocetin and crocin in several cancer cell lines. Crocetin induced cell death at submillimolar concentrations (IC_{50} values ranging from 0.16 to 0.61 mM in a panel of cancer cells). However, crocin proved to be more potent in the cytotoxicity assays (IC_{50} values ranging from 2.87 to 5.48 μM). Both expression and activity of *h*LDH-5 were reduced after treatment of HeLa cells with crocetin and crocin: even in this case, crocetin was more potent than crocin, since crocetin at 1 mM reduced *h*LDH-5 activity by 34.2 % compared to control and crocin reached only a 10.5% inhibition at 4 mM. However, these cell-based experiments did not

determine whether crocetin or crocin directly interact with *h*LDH-5 because various mechanisms could be implicated at the cellular level.[33] It could be predicted that the long carbon chains of these derivatives, characterized by polar moieties (carboxylic groups or sugar portions) at both the extremities, are well tolerated in the LDH active site. These preliminary results encouraged us to carry on further detailed studies in order to clarify the specific effects of crocetin and crocin on *h*LDH-5 and in cancer cells, as described below.

MATERIALS AND METHODS

Chemicals. General Procedures and Materials. All solvents and chemicals were used as purchased without further purification (Aldrich, Alfa Aesar, TCI Europe). The following chemicals were used for the synthesis of the final compounds and were obtained from commercial suppliers: *trans*-2-methyl-2-butenoic acid, methanol, sulfuric acid, diethyl ether, chloroform, *N*-bromosuccinimide, benzoylperoxide (70 %, remainder water), fumaraldehyde mono(dimethylacetal), (carbethoxyethylidene)triphenylphosphorane, triphenylphosphine, activated manganese dioxide, acetone, 1 M diisobutylaluminum hydride solution in anhydrous hexane, Amberlyst® 15 hydrogen form, Celite® Hyflo, ethyl acetate, hexane, dichloromethane (DCM), toluene, acetonitrile, phosphoric acid, sodium hydroxide, sodium sulphate anhydrous, potassium carbonate. Chromatographic separations were performed on silica gel columns by flash chromatography (Kieselgel 40, 0.040−0.063 mm; Merck). Reactions were followed by thin layer chromatography (TLC) on Merck aluminum silica gel (60 F254) sheets that were visualized under a UV lamp. Evaporation was performed in vacuo (rotating evaporator). Sodium sulfate was always used as the drying agent. Proton (^{1}H) and carbon (^{13}C) NMR spectra were obtained with a Bruker Avance III 400 MHz spectrometer using the indicated deuterated solvents. Chemical shifts are given in parts per million (ppm) (δ relative to residual solvent peak for ^{1}H and ^{13}C). ^{1}H-NMR spectra are reported in this order: multiplicity and number of protons. Standard abbreviation indicating the multiplicity were

used as follows: s = singlet, d = doublet, dd = doublet of doublets, ddd = doublet of doublet of doublets, t = triplet, q = quartet, dq = doublet of quartets, tq = triplet of quartets, qq = quartet of quartets, quint = quintet, m = multiplet, bq = broad quartet and bd = broad doublet.

(*E*)-Methyl 2-methylbut-2-enoate (**2**). *Trans*-2-methyl-2-butenoic acid **1** (5.0 g; 50 mmol) was dissolved in MeOH (50 mL) in a sealed vial, concentrated H_2SO_4 (0.27 mL) was added dropwise and the resulting solution was heated at 90 °C for 24 h. The reaction mixture was cooled to room temperature and concentrated under reduced pressure. The resulting mixture was diluted with Et_2O, and then washed successively with a saturated solution of sodium bicarbonate and brine. The organic phase was dried and evaporated under reduced pressure. The crude methyl tiglate **2** was obtained as a light yellow oil (34.1 mmol, yield 63%) and was used in the next step without further purification. ^{1}H NMR ($CDCl_3$) δ (ppm): 1.79 (dq, 3H, *J* = 7.1, 1.2 Hz), 1.83 (quint, 3H, *J* = 1.2 Hz), 3.73 (s, 3H), 6.86 (qq, 1H, *J* = 7.1, 1.4 Hz).

(*E*)-Methyl 4-bromo-2-methylbut-2-enoate (**3**) and (*Z*)-methyl 2-(bromomethyl)but-2-enoate (**4**). Compound **2** (2.0 g; 18 mmol) was dissolved in $CHCl_3$ (23.0 mL), then NBS (18 mmol) and 70% BPO (0.7 mmol) were added and the reaction was heated at reflux for 2 h. After cooling to room temperature, the mixture was concentrated under reduced pressure. Hexane was added to the residue and the resulting suspension was cooled in an ice bath to promote the precipitation of succinimide, which was suction filtered off. The filtrate was evaporated. The residue was diluted with AcOEt and washed with brine. The organic phase was dried and evaporated under vacuum. Mixture of γ and α-bromo derivatives was obtained as an orange oil (3.08 g). ^{1}H NMR ($CDCl_3$) δ (ppm, assigned only significant protons): 3.77 (s, COOMe γ isomer), 3.80 (s, COOMe α isomer), 4.03 (dq, *J* = 8.5, 0.5 Hz, CH_2 γ isomer), 4.24 (s, CH_2 α isomer), 6.93 (tq, *J* = 8.5, 1.5 Hz, vinylic proton γ isomer), 7.08 (q, *J* = 7.3 Hz, vinylic proton α isomer). Proton integration of these signals suggested the following composition: 68 % γ isomer, 32 % α isomer.

(*E*)-(4-Methoxy-3-methyl-4-oxobut-2-en-1-yl)triphenylphosphonium bromide (**5**). Mixture of **3** and **4** (3.08 g) dissolved in toluene (13.7 mL) was treated dropwise with a freshly prepared solution of

triphenylphosphine (21.6 mmol) in toluene (21.0 mL) and the reaction mixture, which became immediately cloudy, was stirred vigorously overnight. A white crystalline solid and a yellow gummy solid adherent to the walls of the flask formed: the white crystalline solid was suction filtered, washed with hexane and dried under vacuum and the yellow gummy solid was dissolved in MeOH and dried under vacuum. Both the fractions were purified by recrystallization from CH_3CN/AcOEt. Compound **5** (2.08 g, 4.57 mmol) was obtained as a white crystalline solid (yield on two subsequent steps: 26 %).^{1}H NMR ($CDCl_3$) δ (ppm): 1.67 (d, 3H, *J* = 3.3 Hz), 3.68 (s, 3H), 5.08 (dd, 2H, *J* = 16.3, 8.0 Hz), 6.64 (bq, 1H, *J* = 6.7 Hz), 7.64-7.94 (m, 15H).

(*E*)-Methyl 2-methyl-4-(triphenylphosphoranylidene)but-2-enoate (**6**). To a solution of phosphonium salt **5** (1.06 g, 2.32 mmol) in CH_2Cl_2 (9.0 mL) was added dropwise aqueous NaOH 0.5 M (4.6 mL) and the mixture became immediately orange. After stirring for 10 minutes, the mixture was diluted with water and extracted with CH_2Cl_2, the organic layer was washed with brine, dried and concentrated under reduced pressure. Crude compound **6** (800 mg, 2.14 mmol) was obtained as an orange oily solid and used in the subsequent steps without further purification (yield 92%).^{1}H NMR ($CDCl_3$) δ (ppm, assigned only significant protons): 1.89 (s, 3H, CH_3), 3.58 (s, 3H, COOMe).

(*2E,4E*)-Ethyl 2-methyl-6-oxohexa-2,4-dienoate (**9**). A solution of fumaraldehyde mono(dimethylacetal) **8** (300 mg; 0.29 mL, 2.31 mmol) in CH_2Cl_2 (3.6 mL) was added dropwise to a solution of (carbethoxyethylidene)triphenylphosphorane **7** (1.09 g; 3.00 mmol) in CH_2Cl_2 (8.9 mL). The reaction was stirred at RT overnight. Solvent was reduced under reduced pressure and then the residue was cooled in an ice bath to promote the precipitation of triphenylphosphine oxide, that was suction filtered off and washed with petroleum ether. The filtrate was concentrated, affording the dimethylacetal product in mixture with the corresponding aldehyde derivative, as a white solid (560 mg). The mixture was directly subjected to the next step without further purification. The residue was dissolved in acetone (9.6 mL), then distilled water (0.15 mL) and Amberlyst 15 (prewashed with acetone, 102 mg) were added and the reaction was stirred for 1 h. After filtration to remove the resin, the filtrate was concentrated and purified by flash chromatography over silica gel (*n*-hexane/Et_2O

85:15). Compound **9** was obtained as a yellow oil (355 mg, 2.11 mmol, yield was calculated on two subsequent steps: 91%). ^{1}H NMR ($CDCl_3$) δ (ppm): 1.33 (t, 3H, *J* = 7.1 Hz), 2.12 (d, 3H, *J* = 1.4 Hz), 4.27 (q, 2H, *J* = 7.1 Hz), 6.39 (dd, 1H, *J* = 15.0, 7.8 Hz), 7.33 (dq, 1H, *J* = 11.8, 1.3 Hz), 7.42 (dd, 1H, *J* = 14.9, 11.8 Hz), 9.70 (d, 1H, *J* = 7.6 Hz).

(*2E*,*4E*,*6E*)-Diethyl 2,7-dimethylocta-2,4,6-trienedioate (**10**). Compound **9** (350 mg, 2.08 mmol) was dissolved in DCM (15.4 mL) and (carbethoxyethylidene)triphenylphosphorane **7** (2.72 mmol) was added. The reaction was stirred at room temperature for 2 h. The mixture was filtered through a Büchner funnel partially filled with silica gel and washed with AcOEt. The filtrate was purified by flash chromatography over silica gel (*n*-hexane/AcOEt 95:5). Compound **10** was obtained as a pearl-white solid (342 mg, 1.36 mmol, yield 65%). ^{1}H NMR ($CDCl_3$) δ (ppm): 1.32 (t, 6H, *J* = 7.1 Hz), 2.01 (d, 6H, *J* = 1.2 Hz), 4.23 (q, 4H, *J* = 7.1 Hz), 6.80 (dd, 2H, *J* = 7.8, 3.1 Hz), 7.28 (dq, 2H, *J* = 7.9, 1.4 Hz).

(*2E*,*4E*,*6E*)-2,7-Dimethylocta-2,4,6-triene-1,8-diol (**11**). Compound **10** (340 mg, 1.35 mmol) was dissolved in anhydrous hexane (10.4 mL) under Argon atmosphere, cooled to -78 °C and treated dropwise with a solution 1 M of DIBAL-H in anhydrous hexane (5.3 mL, 5.26 mmol). The resulting solution was stirred at the same temperature for 5 min and warmed slowly till -20 °C over 3 h. The reaction was monitored by TLC, showing that the diester was completely reacted. The reaction mixture was cooled to 0 °C and distilled water (0.3 mL) and silica gel (900 mg) were added. After 45 minutes, K_2CO_3 (322 mg) and Na_2SO_4 (488 mg) were added. After 30 minutes, the solids were suction filtered off and rinsed with CH_2Cl_2 and AcOEt, the filtrate was concentrated to obtain compound **11** as a light-yellow solid (214 mg, 1.27 mmol, yield 94%) that was used in the next step without further purification. ^{1}H NMR ($CDCl_3$) δ (ppm): 1.82 (s, 6H), 4.11 (s, 4H), 6.16 (dq, 2H, *J* = 7.5, 1.4 Hz), 6.45 (dd, 2H, *J* = 7.3, 3.1 Hz).

(*2E*,*4E*,*6E*)-2,7-Dimethylocta-2,4,6-trienedial (**12**). Compound **11** (214 mg, 1.27 mmol) was dissolved in acetone (11.5 mL) and the solution was cooled to 0 °C. Activated MnO_2 (3.32 g, 38.2 mmol) was added and the reaction was stirred overnight at room temperature. The mixture was

filtered in a Büchner funnel filled with celite Hyflo® and washed with acetone. The filtrate was concentrated under reduced pressure and purified by flash chromatography over silica gel (*n*-hexane/AcOEt 85:15). Compound **12** (152 mg, 0.927 mmol) was obtained as a bright yellow solid (yield 73%). ^{1}H NMR ($CDCl_3$) δ (ppm): 1.95 (d, 6H, *J* = 1.2 Hz), 6.97-7.13 (m, 4H), 9.55 (s, 2H).

(*2E,4E,6E,8E,10E,12E,14E*)-Dimethyl-2,6,11,15-tetramethylhexadeca-2,4,6,8,10,12,14-heptaenedioate (**13**). A solution of compound **6** (1.83 mmol) in toluene (3.5 mL) was added to compound **12** (50.0 mg, 0.305 mmol) in toluene (1.0 mL) and the reaction was heated at 130 °C for 6 h. Then, the mixture was cooled to room temperature and left under stirring overnight. Compound **13** precipitated as a red brick solid, which was collected by filtration and washed with cold MeOH. The filtrate was concentrated under reduced pressure, the residue was taken up in 5 mL of MeOH and heated at 90°C for 30 minutes. The mixture was cooled to room temperature and a second fraction of pure compound **13** was collected. The total amount of pure compound **13** obtained was 61.4 mg (0.172 mmol, yield 56%). ^{1}H NMR ($CDCl_3$) δ (ppm): 1.99 (s, 6H), 2.00 (d, 6H, *J* = 1.0 Hz), 3.77 (s, 6H), 6.34-6.40 (m, 2H), 6.55 (dd, 2H, *J* = 15.2, 10.4 Hz), 6.62 (d, 2H, *J* = 14.8 Hz), 6.71 (dd, 2H, *J* = 7.9, 2.9 Hz), 7.29 (dd, 2H, *J* = 10.7, 1.3 Hz). ^{13}C NMR ($CDCl_3$) δ (ppm): 12.94 (2C), 13.04 (2C), 51.95 (2C), 123.97 (2C), 126.62 (2C), 131.48 (2C), 135.16 (2C), 136.87 (2C), 139.04 (2C), 143.90 (2C), 169.09 (2C).

Sodium (*2E,4E,6E,8E,10E,12E,14E*)-2,6,11,15-tetramethylhexadeca-2,4,6,8,10,12,14-heptaenedioate (**14**) and (*2E,4E,6E,8E,10E,12E,14E*)-2,6,11,15-tetramethylhexadeca-2,4,6,8,10,12,14-heptaenedioic acid (**15**). Diester **13** (25.0 mg, 0.0701 mmol) was suspended in MeOH (0.5 mL) and 40 % w/v NaOH (0.7 mL, 7.01 mmol) was added dropwise. The mixture was heated at reflux overnight. After consumption of the starting material, the mixture was cooled to room temperature and then to 0 °C and an orange precipitated formed. The solid was collected by filtration, washing it with cold water and cold MeOH, affording 21.9 mg (0.588 mmol) of the disodium salt **14** as a bright orange solid (yield 84 %). In order to obtain the diacid **15**, the work-up was accomplished by evaporating the solvent of the reaction, then the residue was diluted with water and the aqueous

phase was washed with Et_2O. The aqueous layer was acidified with 10 % H_3PO_4, to obtain the precipitation of a red solid that was collected and washed with water and CH_2Cl_2 (yield 68 %). For disodium salt **14** ^{1}H NMR (D_2O) δ (ppm): 1.95 (s, 6H), 2.00 (s, 6H), 6.43-6.48 (m, 2H), 6.65-6.70 (m, 4H), 6.85 (dd, 2H, *J* = 7.9, 2.9 Hz), 6.97-7.02 (m, 2H). ^{13}C NMR (D_2O) δ (ppm): 11.92 (2C), 13.42 (2C), 124.86 (2C), 131.13 (2C), 133.37 (2C), 133.96 (2C), 134.85 (2C), 137.31 (2C), 141.46 (2C), 177.94 (2C). For diacid **15** ^{1}H NMR (DMSO-d_6) δ (ppm): 1.91 (s, 6H), 1.97 (s, 6H), 6.43-6.53 (m, 2H), 6.61 (dd, 2H, *J* = 14.8, 11.6 Hz), 6.72 (d, 2H, *J* = 15.2 Hz), 6.78-6.88 (m, 2H), 7.20 (bd, 2H, *J* = 10.8 Hz).

Enzyme assays. The compounds were evaluated in enzymatic assays to assess their inhibitory properties against two commercially available purified human isoforms of lactate dehydrogenase, *h*LDH-5 (tetrameric isoform composed of four A subunits, LDH-A_4, from human liver, Lee BioSolutions – USA) and *h*LDH-1 (tetrameric isoform composed of four B subunits, LDH-B_4, from human erythrocytes, Lee BioSolutions – USA), as suspensions in 3.1 M ammonium sulfate solution, with tris chloride, DTT and EDTA, pH 8.3 Dried flower stigmas (saffron pistils) and crocin were purchased from Sigma-Aldrich. The reaction of lactate dehydrogenase was conducted using the "forward" direction (pyruvate → lactate) by using an emission wavelength at 460 nm and an excitation wavelength at 340 nm to monitor the amount of NADH consumed. These assays were conducted in wells containing 200 µL of a solution comprising the reagents dissolved in 100 mM phosphate buffer at pH 7.4. DMSO stock solutions of compounds were prepared (the concentration of DMSO did not exceed 4% during the measurements). Assays were performed in the presence of 40 µM NADH and 200 µM pyruvate, combined with 0.66 ng or 0.38 mU of enzyme in a final volume of 200 µl (one unit of the enzyme reduces 1 µmol of pyruvate to L-lactate at 37 °C and pH 8.55). Seven different concentrations (in duplicate for each concentration) of the compound were used to generate a concentration–response curve. Compound solutions were dispensed in 96-well plates (8 µL), and then the substrate and the cofactor dissolved in the buffer (152 µL) and the enzyme solution (40 µL) were added. Any possible background fluorescence of the tested compounds, or their

quenching of NADH fluorescence, was subtracted. In addition to the compound test wells, each plate contained maximum and minimum controls. Assay plates were incubated for 15 min, and the final measurements were performed using a Victor X3 Microplates Reader (PerkinElmer®). IC50 values were generated using the curve-fitting tool of GraphPad Prism software (GraphPad – USA). In the enzyme kinetic experiments, the same procedure previously reported by us was followed.[13] The compound was tested in the presence of scalar NADH or pyruvate concentrations in the NADH or pyruvate-competition experiments, respectively. In the NADH-competition experiments, the compound was added (concentration range = 15-45 μM) to a reaction mixture containing 1.4 mM pyruvate, scalar concentrations of NADH (concentration range = 10–150 μM) and 100 mM phosphate buffer (pH = 7.4). Conversely, in the pyruvate-competition experiments, the reaction mixture contained 150 μM NADH and scalar concentrations of pyruvate (concentration range = 40–500 μM). Finally, LDH solution was added (0.015 U/mL) and the enzyme activity was measured by evaluating the NADH fluorescence decrease using a Victor X3 Microplates Reader. The experimental data were analysed with a non-linear regression analysis, using a second order polynomial regression analysis, and by applying the mixed-model inhibition fit.

Cell lines and cell culture. A549 cell lines were obtained from ATCC and grown in RPMI 1640 medium with 10 % fetal bovine serum, 100 U/mL penicillin, and 100 μg/mL streptomycin. HeLa cell lines were obtained from ATCC and grown in EMEM with 10 % fetal bovine serum, 100 U/mL penicillin, and 100 μg/mL streptomycin. Cells were cultured at 37 °C in a 5 % CO2– 95% air humidified atmosphere.

Cytotoxicity evaluation. HeLa and A549 cells were seeded on 96 well plates at the density of 1 x 10^3 cells per well. The cells were continuously treated with various concentrations of compound **14** for 72 h. Then viability was assessed using the sulforhodamine B (SRB) assay. Cells were fixed with 10% trichloroacetic acid at 4 °C for overnight and then stained with 0.057% SRB in 1 % acetic acid at room temperature for 30 min. The dye was solubilized in 10 mM Tris base (pH 10.5) and absorption at 510 nm was measured using a SpectraMax Plus 384 (Molecular Devices, Sunnyvale, CA). Percent

death was calculated by subtracting background from all wells and setting 0% death to vehicle-treated controls. All data are averages of at least three independent replicates. MRC5 cells (from ATCC) were maintained at 37 °C in a humidified atmosphere containing 5% CO_2 accordingly to the supplier. Normal (1.5×10^4) cells were plated in 96-well culture plates. The day after seeding, vehicle or compound were added at different concentrations to the medium. Cell viability was measured after 96 h according to the supplier (Promega, G7571) with a Tecan F200 instrument. IC_{50} values were calculated from logistical dose response curves. Averages were obtained from three independent experiments, and error bars are standard deviations (n = 3).

Assessment of lactate production. HeLa human cervical carcinoma cells were seeded on 96 well plates at the density of 2.5 x 10^3 cells per well. When cells reached 80-90 % confluence, the cells were treated with compound or vehicle control in DMEM medium minus phenol red + 10% dialized FBS + 100 U/mL penicilin + 100 µg/mL streptomycin for 4 h. Triplicate wells were prepared for each treatment. Following treatment, the cells were fixed with 10 % trichloroacetic acid for the assessment of cell viability using SRB assay and the media were collected, and 100 µL were added to 10 µL 10 mM chlorophenylalanine (CPA; the internal standard for GC-MS analysis). Samples were concentrated, derivatized by a 2h incubation with 50 µL MTBSTFA + 1% TBDMCS (Thermo Scientific, Walthman, MA) in 50 µL acetonitrile at 80 °C, and immediately analyzed using GC-MS (Agilent 6890N GC/5973 MS, equipped with an Agilent DB-5 capillary column, 30 m x 320 µm x 0.25 µm, model number J&W 123-5032, Agilent Technologies, Santa Clara, CA) and electron impact ionization source. The initial oven temperature was 120 °C, held for 5 min; then the temperature was increased at a rate of 10 °C per minute until a temperature of 250 °C was reached. The temperature was then increased by 40 °C per minute until a final temperature of 310 °C was reached. The total run time per sample was 24.5 min. Compounds were identified using AMDIS Chromatogram software (Amdis, freeware available from amdis.net) and programmed WIST and Niley commercial libraries. The integration area of lactate in each sample was divided by the integration area of CPA in the same sample to achieve a lactate/internal standard ratio. The ratios were normalized by % live

and averaged for triplicates. The percentage lactate production over vehicle was calculated and all data are averages of three independent replicates.

Statistical Analysis. All statistical analysis was performed using an unpaired, two-tailed student's t test with p values < 0.05 were considered statistically significant. Values are reported as the means ± SD of three or more independent experiments.

Docking Calculations. The crystal structure of the *h*LDH-5 protein (4M49 PDB code[34]), was taken from the Protein Data Bank.[35] After adding hydrogen atoms, the protein was minimized using Amber14 software and the ff14SB force field at 300 K (in order to reproduce the room temperature used in the enzymatic assay).. The complex was placed in a rectangular parallelepiped waterbox, an explicit solvent model for water, TIP3P, was used and the complex was solvated with a 10 Å water cap. Sodium ions were added as counterions to neutralize the system. Two steps of minimization were then carried out; in the first stage, we kept the protein fixed with a position restraint of 500 kcal/molÅ^2 and we solely minimized the positions of the water molecules. In the second stage, we minimized the entire system through 5000 steps of steepest descent followed by conjugate gradient (CG) until a convergence of 0.05 kcal/Åmol. The ligands were built using Maestro and were minimized by means of Macromodel in a water environment using the CG method until a convergence value of 0.05 kcal/Åmol, using the MMFFs force field and a distance-dependent dielectric constant of 1.0. AUTODOCK Tools,[36] was used to define the torsion angles in the ligands, to add the solvent model and to assign partial atomic charges to the ligand and the protein. The docking site used for AUTODOCK calculations was defined in such a manner that it was constituted by all residues within 10 Å of the reference ligand and NADH co-factor in the X-ray crystal structure. The energetic maps were calculated using a grid spacing of 0.375 Å and a distance dependent function of the dielectric constant. The ligand was subjected to 200 docking runs of the AUTODOCK search using the Lamarckian genetic algorithm (LGA) and employing 10 000 000 energy evaluations; the number of individuals in the initial population was set to 500 and a maximum of 10 000 000 generations were

simulated during the docking run; an rms tolerance of 2.0 Å was used to carry out the cluster analysis of the docking solutions and all the other settings were left as their defaults.

MD simulations. All simulations were performed using AMBER, version 14.[37] MD simulations were carried out using the ff14SB force field at 300 K. The complex was placed in a rectangular parallelepiped water box. An explicit solvent model for water, TIP3P, was used, and the complexes were solvated with a 20 Å water cap. Chlorine ions were added as counterions to neutralize the system. Prior to MD simulations, two steps of minimization were carried out using the same procedure described above. Particle mesh Ewald (PME) electrostatics and periodic boundary conditions were used in the simulation.[38] The MD trajectory was run using the minimized structure as the starting conformation. The time step of the simulations was 2.0 fs with a cutoff of 10 Å for the nonbonded interaction, and SHAKE was employed to keep all bonds involving hydrogen atoms rigid. Constant-volume periodic boundary MD was carried out for 0.5 ns, during which the temperature was raised from 0 to 300 K. Then 19.5 ns of constant pressure periodic boundary MD was carried out at 300 K using the Langevin thermostat to maintain constant the temperature of our system. All the α carbons of the protein were blocked with a harmonic force constant of 10 kcal/mol•Å^2 for the first 3.5 ns. General Amber force field (GAFF) parameters were assigned to the ligand, while partial charges were calculated using the AM1-BCC method as implemented in the Antechamber suite of AMBER 14. The final structures of the complexes were obtained as the average of the last 16.5 ns of MD minimized by the CG method until a convergence of 0.05 kcal/mol•Å^2. The average structures were obtained using the Cpptraj program[39] implemented in AMBER 14.

Binding Energy Evaluation. The evaluation of the binding energy associated to the different ligand-protein complexes analyzed through MD simulations was carried out using AMBER 14. The trajectories relative to the last 16.5 ns of each simulation were extracted and used for the calculation, for a total of 165 snapshots (at time intervals of 100 ps). Van der Waals, electrostatic and internal interactions were calculated with the SANDER module of AMBER 14, whereas polar energies were calculated using both the Generalized Born and the Poisson−Boltzman methods with the MM-PBSA

module of AMBER 14. Dielectric constants of 1 and 80 were used to represent the gas and water phases, respectively, while the MOLSURF program was employed to estimate the nonpolar energies. The entropic term was considered as approximately constant in the comparison of the ligand−protein energetic interactions.

RESULTS AND DISCUSSION

LDH inhibition assays of saffron polar extract

Commercially available red stigmatic lobes of saffron were dissolved in a suitable polar solvent, such as dimethyl sulfoxide (DMSO), and the polar saffron chemical constituents were extract, which we hypothesized would have a higher chance to efficiently interact with the highly hydrophilic catalytic site of *h*LDH-5 than non-polar components. The saffron DMSO extract was then serially diluted and tested on *h*LDH-5 and *h*LDH-1 purified isoforms to determine its inhibition potency. At the maximum tested concertation of 0.8 mg/mL, we observed an inhibition of 52% of the activity of *h*LDH-5 (corresponding to an IC_{50} value of 0.653 mg/mL) and of 49% of the activity of *h*LDH-1 (resulting in an IC_{50} value of 0.717 mg/mL) by the saffron solution. The noticeable activity of the crude saffron polar extract a served as the starting point for the investigation into this dietary natural product and the identification of the constituents responsible for the inhibition of LDH enzymes.

Chemical synthesis of crocetin

Unlike crocin, which is commercially available at a reasonable level of purity, it was not possible to easily purchase or extract crocetin in sufficient purity and amount to complete further biological studies. Therefore, crocetin was synthesized by a multi-step synthesis. Crocetin possesses a diterpenic and symmetrical structure, possessing alternating *trans* double bonds in the alkyl chain, four methyl groups and carboxylic groups at both ends of the backbone. The synthesis of this carotenoid required the formation of two fragments that converged in the last steps: 1) synthesis of the central dialdehyde

unsaturated carbon chain (compound **12**, Scheme 1, part B) and 2) formation of a triphenylphosphoranylide intermediate (compound **6**, Scheme 1, part A), which would be condensed at both the terminal parts of the previous chain.[40] The first part of this synthetic pattern was the preparation of (*E*)-methyl 2-methyl-4-(triphenylphosphoranylidene)but-2-enoate **6**, which was condensed with dialdehyde **12** to obtain dimethyl crocetinate **13**, an immediate precursor of crocetin (Scheme 1). Initially, a methanolic solution of *trans*-2-methyl-2-butenoic acid **1**, also called tiglic acid, was heated in the presence of H_2SO_4 to obtain the methyl tiglate **2** (Scheme 1). Methyl tiglate is a highly volatile compound, so it was necessary to take some precautions: *a*) the reaction was performed in a sealed vial in order to minimize the evaporation of the product during heating, and *b*) the workup procedure avoided exposing this intermediate to a high vacuum. The product was obtained as a crude light yellow oil that was subsequently used in the next step without further purification. Methyl ester **2** was subjected to a radical bromination with *N*-bromosuccinimide (NBS) in the presence of the radical initiator benzoyl peroxide (BPO), which afforded a mixture of the two possible regioisomers, γ and α allylic bromides (compounds **3** and **4**, respectively). The relative amounts of the two regioisomers were evaluated by ^{1}H-NMR (signals of methylene protons, see experimental section) and γ and α bromides were present in a 3:2 ratio, respectively. The mixture was used in the next step without further purification. The mixture of compounds **3** and **4** was dissolved in toluene and combined with a slight excess of triphenylphosphine to get phosphonium salts. At this time, the triphenylphosphonium salt of methyl γ-bromotiglate **5** was isolated as a pure regioisomer by recrystallization from CH_3CN/AcOEt (Scheme 1). Compound **5** was treated with aqueous sodium hydroxide to afford compound **6**. However the formed triphenylphosphoranylide proved to be particularly instable upon exposure to atmospheric oxygen. These observations led us to perform the reaction under an Argon atmosphere and avoid purification of this compound. The reaction was monitored via the presence of representative signals in the ^{1}H-NMR spectrum (see experimental section) and compound **6** was prepared immediately before its use in the subsequent Wittig reaction (Scheme 1).

The second fragment of the synthesis involved the preparation of dialdehyde **12** (Scheme 1), which was to be condensed with phosphoranylide **6**. The synthesis of **12** commenced with a Wittig reaction between commercially available fumaraldehyde mono(dimethyl acetal) **8** and (carbethoxyethylidene)triphenylphosphorane **7**, providing a mixture of both the desired condensation product still possessing the dimethyl acetal portion (structure not shown) and condensation product **9** possessing the free aldehyde moiety. This resulted the acetal group being partially removed under these reaction conditions. Considering that the next step of the synthesis involved the deprotection of the acetal moiety to obtain aldehyde **9**, the mixture was treated with amberlyst 15 in a biphasic solvent system consisting of water and acetone, which lead to the complete hydrolysis of the dimethyl acetal group to afford pure aldehyde **9**. Amberlyst 15 was used as an acid catalyst due to its not affecting the highly reactive double bonds present in the structure of the starting material and its ease of purification. A second Wittig reaction with (carbethoxyethylidene)triphenylphosphorane **7** gave the symmetric diester intermediate **10**. Compound **10** was then reduced to form the corresponding dialcohol **11** via an excess of diisobutylaluminum hydride (DIBAL-H) and anhydrous hexane as solvent. The subsequent partial oxidation of the allylic alcoholic groups of compound **11** was performed with MnO_2 to give the corresponding dialdehyde **12**. Compound **12** was subjected to a double Wittig reaction with the triphenylphosphoranylide **6**, thus extending the unsaturated carbon chain at both terminals. The resulting dimethyl ester of crocetin **13** precipitated as a red powder and was isolated by filtration. The precipitate was recrystallized from MeOH to obtaine material of sufficient purity. Compound **13** was saponified with aqueous NaOH to give the corresponding sodium salt (disodium crocetinate **14),** which precipitated as a bright orange solid (step g, Scheme 1). Alternatively, the saponification was followed by acidification with phosphoric acid to obtain the free diacid crocetin **15** (step h, Scheme 1).[41]

LDH inhibition assays of crocetin and crocin

Synthetic dibasic crocetin (compound **14**), its dimethyl ester precursor **13**, and commercially available crocin **16** were tested on *h*LDH-5 and *h*LDH-1 purified isoforms to determine their inhibitory properties, relative to galloflavin, which served as a positive control (Table 1).[12] The disodium salt **14** was preferred to free acid **15** in these biological assays, since the salt form readily dissolved in the aqueous buffer without any additional organic solvent. Nevertheless, crocetin as diacid (**15**) was tested to confirm the inhibitory activity on the enzyme. Compound **13** was found to be completely inactive, displaying IC_{50} values greater than 200 μM for both isoforms. Conversely, disodium salt **14**, showed noticeable inhibition of *h*LDH-5 (IC_{50} = 54.9 μM) and it was selective for this isoform, proving to be less active on isoform 1 (IC_{50} > 200 μM). The IC_{50} value of diacid **15** nicely overlaps with that of its disodium salt (Table 1). Reference inhibitor galloflavin was 1.7-fold less potent than compound **14**, and it also inhibited isoform 1 of the enzyme with a similar potency. Crocin **16** was less effective in the inhibition of *h*LDH-5 relative to crocetin, with an IC_{50} value similar to that of galloflavin (IC_{50} = 95.7 μM), and it showed selectivity towards isoform 1 (IC_{50} = 59.8 μM). In order to complete the biochemical characterization of crocetin, a kinetic assay was performed by applying a mixed-model inhibition fit to the second order polynomial regression analysis of the rate of conversion of NADH to NAD^+ to obtain K_i values in the NADH-competition experiments. In these experiments we measured an apparent Michaelis–Menten constant (K_M) of 20 μM and a K_i value of 25.6 μM, which is consistent with the IC_{50} values of both forms of crocetin (disodium salt **14** and diacid **15**) reported in Table 1. Similarly, in the pyruvate-competition experiments in which the K_M value was of 100 μM, the resulting K_i value was of 21.1 μM.

From a structural point of view, we can conclude that the replacement of the two carboxylic acids of crocetin by methyl ester groups, as in compound **13**, or the esterification with sugar moieties, as in crocin **16**, led to a loss of inhibitory activity (in the case of **13**) or a slight decrease in activity and a marked loss of selectivity for isoform 5 (in the case of **16**), thus identifying crocetin as the most active compound among these saffron derivatives.

Inhibition of cancer cell proliferation and reduction of cellular lactate production

Following the results previously obtained with isolated LDH enzyme isoforms, studies in cancer cells were focused on the disodium salt of crocetin **14** because it was found to be the most active *h*LDH-5 inhibitor among the saffron derivatives herein studied. Compound **14** was evaluated for growth inhibitory effects on two different cancer cell lines, HeLa (human cervical carcinoma cells) and A549 (human lung carcinoma cells), after 72 hours of incubation. Cell death was assessed by Sulforhodamine B (SRB) staining, as previously described[42] and the cytotoxic potency of the tested compound was expressed as IC_{50} values, which represent the concentration of a compound that is required for the 50% inhibition of cell proliferation. Compound **14** was able to counteract cancer cell growth both in A549 and in HeLa cells with similar IC_{50} values of 114.0 ± 8.0 and 113.0 ± 11.1 μM, respectively (Figure 3, panel A), which may be considered as respectable values for a food component. Furthermore, **14** proved to be completely inactive against noncancerous human fibroblast lung cells (MRC5 IC_{50} > 500 μM).After the preliminary biochemical evaluation on the isolated enzymes and the cytotoxicity assays on two cancer cell lines, this compound was also assayed for its ability to inhibit the production of lactate in cancer cells. To this end, HeLa cells were treated with **14** in phosphate buffer saline (PBS) for 6 hours and then the cell culture medium was extracted and mixed with a known amount of chlorophenylalanine (CPA, internal standard) and dried. Concentrated samples were reacted with *N*-methyl-*N*-*tert*-butyldimethylsilyltrifluoroacetamide (MTBSTFA) for derivatization of lactate, which was needed for its GC-MS detection and quantification. The cells were fixed and biomass was measured using SRB. Crocetin disodium salt **14** was tested at a 100 μM concentration. As previously reported, the GC-MS analysis of cell culture media for the quantitative determination of extracellular lactate was preferred over other methods, since it allows a highly sensitive determination of low micromolar lactate concentrations.[43] As shown in Figure 3 (Panel B), compound **14** reduced lactate production of about 20 % compared to PBS control at 100 μM after 6 h incubation.

Molecular modelling studies

To rationalize how compound **14** can interact with the *h*LDH-5 protein, molecular docking studies followed by molecular dynamic (MD) simulations and binding energy determinations were carried out. Compound **14** was docked into the crystal structure of the *h*LDH-5 protein (4M49 PDB code) using AUTODOCK software.[36] The 200 different docking results generated were clustered using a root-mean square deviation (RMSD) threshold of 2.0 Å and the so obtained 5 clusters of solutions were considered for further studies (see the Experimental section for details). For each cluster, the docking pose associated with the best estimated binding energy was selected as a representative binding mode. The stability of the 5 different binding modes was then assessed through 20 ns of MD simulation studies with explicit water molecules, as described in the Experimental section. The 5 MD trajectories obtained in this way were further analyzed through the Molecular Mechanics - Poisson Bolzmann Surface Area (MM-PBSA) method,[44] which was shown to accurately estimate the ligand-receptor energy interaction.[45,46] This approach averages the contributions of gas phase energies, solvation free energies, and solute entropies calculated for snapshots of the complex molecule as well as the unbound components extracted from MD trajectories, according to the procedure fully described in the Experimental section. The MM-PBSA results (Table 2) suggest that there is one docking pose that is the most favorable, as it shows an interaction energy ΔPBSA = -29.2 kcal/mol, more than 8 kcal/mol higher than all the other binding poses (docking pose 1, Table 2).

Figure 4 shows the energy minimized average structures of the last 16.5 ns of *h*LDH-5 complexed with the hypothesized binding pose of compound **14**. The ligand interacts within the pyruvate binding site and points towards the binding site entrance. One of the two carboxylic groups forms a hydrogen bond with the catalytic H193, whereas the second carboxylic end forms a strong ionic couple with positively charged residue K57. Although the binding of the compound to the enzyme active site is mainly driven by the interactions of the two carboxylic ends, the internal carbon chain of the ligand also shows lipophilic interactions along the *h*LDH-5 surface and, in particular, with A30, V31, V136 and I252, which represent fundamental additive contributions to the binding process.

In conclusion, an investigation into the bioactive properties of saffron extract led to the discovery of LDH-inhibitory activity, to carotenoid crocetin. Additionally, these compounds mitigated proliferation of glycolytic cancer cells. In order to unambiguously establish the effective activity of this natural compound, a multi-step chemical synthesis was implemented for the production of pure crocetin. Its moderate inhibition potency against the isolated LDH-enzyme, which frankly cannot compete with several synthetic inhibitors previously described, should not be considered as a limiting factor since crocetin is part of a spice (saffron) utilized in aliments, whose relative safety has been now established by millennia of culinary tradition employing it in many recipes. It should be acknowledged the oral LD_{50} for saffron in mice was found to be 20 g/kg, although oral administration of the saffron extract at concentrations from 0.1 to 5 g/kg was demonstrated to be non-toxic in mice.[47] Furthermore, a recent study revealed that administration of up to 400 mg / day of saffron for 1 week to healthy human volunteers did not cause any clinically significant effects,[48] thus confirming its higher safety when compared to classical anticancer drugs. For these reasons, this study contributes to appreciate the role of saffron in the prevention and treatment of cancer when utilized in combination with standard-of-care preventive and therapeutic options.

ACKNOWLEDGEMENTS

We are grateful to the NIH grants R01-GM098453 (to PJH and FM), the University of Pisa, and the University of Illinois for support of this work.

REFERENCES

1. Warburg, O. On the origin of cancer cells. *Science* **1956**, *123*, 309-314.
2. Granchi, C.; Minutolo, F. Anticancer agents that counteract tumor glycolysis. *ChemMedChem* **2012**, *7*, 1318-1350.
3. Granchi, C.; Fancelli, D.; Minutolo, F. An update on therapeutic opportunities offered by cancer glycolytic metabolism. *Bioorg. Med. Chem. Lett.* **2014**, *24*, 4915-4925.
4. Kanno, T.; Sudo, K.; Maekawa, M.; Nishimura, Y.; Ukita, M.; Fukutake, K. Lactate dehydrogenase M-subunit deficiency: a new type of hereditary exertional myopathy. *Clin. Chim. Acta* **1989**, *173*, 89-98.
5. Fantin, V. R.; St-Pierre, J.; Leder, P. Attenuation of LDH-A expression uncovers a link between glycolysis, mitochondrial physiology, and tumor maintenance. *Cancer Cell* **2006**, *9*, 425-434.
6. Granchi, C.; Paterni, I.; Rani, R.; Minutolo, F. Small-molecule inhibitors of human LDH5. *Future Med. Chem.* **2013**, *5*, 1967-1991.
7. Gomez, M. S.; Piper, R. C.; Hunsaker, L. A.; Royer, R. E.; Deck, L. M.; Makler, M. T.; Vander Jagt, D. L. Substrate and cofactor specificity and selective inhibition of lactate dehydrogenase from the malarial parasite P. falciparum. *Mol. Biochem. Parasitol.* **1997**, *90*, 235-246.
8. Wang, Z.; Wang, D.; Han, S.; Wang, N.; Mo, F.; Loo, T. Y.; Shen, J.; Huang, H.; Chen, J. Bioactivity-guided identification and cell signaling technology to delineate the lactate dehydrogenase A inhibition effects of Spatholobus suberectus on breast cancer. *PLoS One* **2013**, *8*, e56631.
9. Arora, R.; Schmitt, D.; Karanam, B.; Tan, M.; Yates, C.; Dean-Colomb W. Inhibition of the Warburg effect with a natural compound reveals a novel measurement for determining the metastatic potential of breast cancers. *Oncotarget* **2015**, *6*, 662-678.
10. Ramanathan, R.; Mancini, R. A.; Suman, S. P.; Beach, C. M. Covalent binding of 4-hydroxy-2-nonenal to lactate dehydrogenase decreases NADH formation and metmyoglobin reducing activity. *J. Agric. Food Chem.* **2014**, *62*, 2112-2117.
11. Deiab, S.; Mazzio, E.; Eyunni, S.; McTier, O.; Mateeva, N.; Elshami, F.; Soliman, K. F. 1,2,3,4,6-Penta-O-galloylglucose within Galla Chinensis Inhibits Human LDH-A and Attenuates Cell Proliferation in MDA-MB-231 Breast Cancer Cells. *Evid. Based Complement. Alternat. Med.* **2015**, *2015*, 276946.
12. Manerba, M.; Vettraino, M.; Fiume, L.; Di Stefano, G.; Sartini, A.; Giacomini, E.; Buonfiglio, R.; Roberti, M.; Recanatini, M. Galloflavin (CAS 568-80-9): a novel inhibitor of lactate dehydrogenase. *ChemMedChem* **2012**, *7*, 311-317.
13. Bader, A.; Tuccinardi, T.; Granchi, C.; Martinelli, A.; Macchia, M.; Minutolo, F.; De Tommasi, N.; Braca, A. Phenylpropanoids and flavonoids from Phlomis kurdica as inhibitors of human lactate dehydrogenase. *Phytochemistry* **2015**, *116*, 262-268.
14. Deiab, S.; Mazzio, E.; Messeha, S.; Mack, N.; Soliman, K. F. High-Throughput Screening to Identify Plant Derived Human LDH-A Inhibitors. *Eur. J. Med. Plants* **2013**, *3*, 603-615.
15. Bathaie, S. Z.; Mousavi, S. Z. New applications and mechanisms of action of saffron and its important ingredients. *Crit. Rev. Food Sci.* Nutr. **2010**, *50*, 761-786.
16. Christodoulou, E.; Kadoglou, N. P.; Kostomitsopoulos, N.; Valsami, G. Saffron: a natural product with potential pharmaceutical applications. *J. Pharm. Pharmacol.* **2015**, *67*, 1634-1649.
17. Geromichalos, G. D.; Lamari, F. N.; Papandreou, M. A.; Trafalis, D. T.; Margarity, M.; Papageorgiou, A.; Sinakos, Z. Saffron as a source of novel acetylcholinesterase inhibitors:

molecular docking and in vitro enzymatic studies. *J. Agric. Food. Chem.* **2012**, *60*, 6131-618.

18. Ahrazem, O.; Rubio-Moraga, A.; Nebauer, S. G.; Molina, R. V.; Gómez-Gómez, L. Saffron: Its Phytochemistry, Developmental Processes, and Biotechnological Prospects. *J. Agric. Food Chem.* **2015**, *63*, 8751-8764.
19. Cossignani, L.; Urbani, E.; Simonetti, M. S.; Maurizi, A.; Chiesi, C.; Blasi, F. Characterisation of secondary metabolites in saffron from central Italy (Cascia, Umbria). *Food Chem.* **2014**, *143*, 446-451.
20. Nescatelli, R.; Carradori, S.; Marini, F.; Caponigro, V.; Bucci, R.; De Monte, C.; Mollica, A.; Mannina, L.; Ceruso, M.; Supuran, C.T.; Secci, D. Geographical characterization by MAE-HPLC and NIR methodologies and carbonic anhydrase inhibition of Saffron components. *Food Chem.* **2017**, *221*, 855-863.
21. Lu, P.; Lin, H.; Gu, Y.; Li, L.; Guo, H.; Wang, F.; Qiu, X. Antitumor effects of crocin on human breast cancer cells. *Int. J. Clin. Exp. Med.* **2015**, *8*, 20316-20322.
22. Chen, S.; Zhao, S.; Wang, X.; Zhang, L.; Jiang, E.; Gu, Y.; Shangguan, A. J.; Zhao, H.; Lv, T.; Yu, Z. Crocin inhibits cell proliferation and enhances cisplatin and pemetrexed chemosensitivity in lung cancer cells. *Transl. Lung Cancer Res.* **2015**, *4*, 775-783.
23. Xia, D. Ovarian cancer HO-8910 cell apoptosis induced by crocin in vitro. *Nat. Prod. Commun.* **2015**, *10*, 249-252.
24. D'Alessandro, A. M.; Mancini, A.; Lizzi, A. R.; De Simone, A.; Marroccella, C. E.; Gravina, G. L.; Tatone, C.; Festuccia, C. Crocus sativus stigma extract and its major constituent crocin possess significant antiproliferative properties against human prostate cancer. *Nutr. Cancer* **2013**, *65*, 930-942.
25. Gutheil, W. G.; Reed, G.; Ray, A.; Anant, S.; Dhar, A. Crocetin: an agent derived from saffron for prevention and therapy for cancer. *Curr. Pharm. Biotechnol.* **2012**, *13*, 173-179.
26. Li, S.; Jiang, S.; Jiang, W.; Zhou, Y.; Shen, X. Y.; Luo, T.; Kong, L. P.; Wang, H. Q. Anticancer effects of crocetin in human esophageal squamous cell carcinoma KYSE-150 cells. *Oncol. Lett.* **2015**, *9*, 1254-1260.
27. Festuccia, C.; Mancini, A.; Gravina, G. L.; Scarsella, L.; Llorens, S.; Alonso, G. L.; Tatone, C.; Di Cesare, E.; Jannini, E. A.; Lenzi, A.; D'Alessandro, A. M.; Carmona, M. Antitumor effects of saffron-derived carotenoids in prostate cancer cell models. *BioMed Res. Int.* **2014**, *2014*, 135048.
28. He, K.; Si, P.; Wang, H.; Tahir, U.; Chen, K.; Xiao, J.; Duan, X.; Huang, R.; Xiang, G. Crocetin induces apoptosis of BGC-823 human gastric cancer cells. *Mol. Med. Rep.* **2014**, *9*, 521-526.
29. Bathaie, S. Z.; Hoshyar, R.; Miri, H.; Sadeghizadeh, M. Anticancer effects of crocetin in both human adenocarcinoma gastric cancer cells and rat model of gastric cancer. *Biochem. Cell Biol.* **2013**, *91*, 397-403.
30. Asai, A.; Nakano, T.; Takahashi, M.; Nagao, A. Orally administered crocetin and crocins are absorbed into blood plasma as crocetin and its glucuronide conjugates in mice. *J. Agr. Food Chem.* **2005**, *53*, 7302-7306.
31. Caballero-Ortega, H.; Pereda-Miranda, R.; Abdullaev, F. I. HPLC quantification of major active components from 11 different saffron (*Crocus sativus* L.) sources. *Food Chem.* **2007**, *100*, 1126-1131.
32. Umigai, N.; Murakami, K.; Ulit, M.; Antonio, L.; Shirotori, M.; Morikawa, H.; Nakano, T. The pharmacokinetic profile of crocetin in healthy adult human volunteers after a single oral administration. *Phytomedicine* **2011**, *18*, 575-578.

33. Kim, S. H.; Lee, J. M.; Kim, S. C.; Park, C. B.; Lee, P. C. Proposed cytotoxic mechanisms of the saffron carotenoids crocin and crocetin on cancer cell lines. *Biochem. Cell Biol.* **2014**, *92*, 105-111.
34. Fauber, B. P.; Dragovich, P. S.; Chen, J.; Corson, L. B.; Ding, C. Z.; Eigenbrot, C.; Giannetti, A. M.; Hunsaker, T.; Labadie, S.; Liu, Y.; Malek, S.; Peterson, D.; Pitts, K.; Sideris, S.; Ultsch, M.; VanderPorten, E.; Wang, J.; Wei, B.; Yen, I.; Yue, Q. Identification of 2-amino-5-aryl-pyrazines as inhibitors of human lactate dehydrogenase. *Bioorg. Med. Chem. Lett.* **2013**, *23*, 5533-5539.
35. Berman, H. M.; Westbrook, J.; Feng, Z.; Gilliland, G.; Bhat, T. N.; Weissig, H.; Shindyalov, I. N.; Bourne, P. E. The Protein Data Bank. *Nucleic Acids Res.* **2000**, *28*, 235-242.
36. Morris, G. M.; Huey, R.; Lindstrom, W.; Sanner, M. F.; Belew, R. K.; Goodsell, D. S.; Olson, A. J. AutoDock4 and AutoDockTools4: Automated docking with selective receptor flexibility. *J. Comput. Chem.* **2009**, *30*, 2785-2791.
37. Case, D. A.; Berryman, J. T.; Betz, R. M.; Cerutti, D. S.; Cheatham, T. E., III; Darden, T. A.; Duke, R. E.; Giese, T. J.; Gohlke, H.; Goetz, A. W.; Homeyer, N.; Izadi, S.; Janowski, P.; Kaus, J.; Kovalenko, A.; Lee, T. S.; LeGrand, S.; Li, P.; Luchko, T.; Luo, R.; Madej, B.; Merz, K. M.; Monard, G.; Needham, P.; Nguyen, H.; Nguyen, H. T.; Omelyan, I.; Onufriev, A.; Roe, D. R.; Roitberg, A.; Salomon-Ferrer, R.; Simmerling, C. L.; Smith, W.; Swails, J.; Walker, R. C.; Wang, J.; Wolf, R. M.; Wu, X.; York, D. M.; Kollman, P. A. AMBER, version 14; University of California: San Francisco, CA, **2015**.
38. York, D. M.; Darden, T. A.; Pedersen, L. G. The Effect of Long-Range Electrostatic Interactions in Simulations of Macromolecular Crystals - a Comparison of the Ewald and Truncated List Methods. *J. Chem. Phys.* **1993**, *99*, 8345-8348.
39. Roe, D. R.; Cheatham, T. E., 3rd. PTRAJ and CPPTRAJ: Software for Processing and Analysis of Molecular Dynamics Trajectory Data. *J. Chem. Theory Comput.* **2013**, *9*, 3084-3095.
40. Gainer, J. L.; Grabiak, R. C. Bipolar trans carotenoid salts and their uses. US2014051759, **2014**.
41. Van Calsteren, M-R.; Bissonnette, M. C.; Cormier, F.; Dufresne, C.; Ichi, T.; LeBlanc, J. C. Y.; Perreault, D.; Roewer, I. Spectroscopic Characterization of Crocetin Derivatives from Crocus sativus and Gardenia jasminoides. *J. Agric. Food Chem.* **1997**, *45*, 1055-1061.
42. Vichai, V.; Kirtikara, K. Sulforhodamine B colorimetric assay for cytotoxicity screening. *Nat. Protoc.* **2006**, *1*, 1112-1116.
43. a) Granchi, C.; Calvaresi, E. C.; Tuccinardi, T.; Paterni, I.; Macchia, M.; Martinelli, A., Hergenrother, P. J.; Minutolo, F. Assessing the differential action on cancer cells of LDH-A inhibitors based on the N-hydroxyindole-2-carboxylate (NHI) and malonic (Mal) scaffolds. *Org. Biomol. Chem.* **2013**, *11*, 6588-6596; b) Calvaresi, E. C.; Granchi, C.; Tuccinardi, T.; Di Bussolo, V.; Huigens, R. W. 3rd.; Lee, H. Y.; Palchaudhuri, R.; Macchia, M.; Martinelli, A.; Minutolo, F.; Hergenrother, P. J. Dual targeting of the Warburg effect with a glucose-conjugated lactate dehydrogenase inhibitor. *Chembiochem.* **2013**, *14*, 2263-2267; c) Di Bussolo, V.; Calvaresi, E. C.; Granchi, C.; Del Bino, L.; Frau, I.; Lang, M. C.; Tuccinardi, T.; Macchia, M.; Martinelli, A.; Hergenrother, P. J.; Minutolo, F. Synthesis and biological evaluation of non-glucose glycoconjugated N-hydroyxindole class LDH inhibitors as anticancer agents. *RSC Adv.* **2015**, *5*, 19944-19954.
44. Kollman, P. A.; Massova, I.; Reyes, C.; Kuhn, B.; Huo, S.; Chong, L.; Lee, M.; Lee, T.; Duan, Y.; Wang, W.; Donini, O.; Cieplak, P.; Srinivasan, J.; Case, D. A.; Cheatham, T. E.

3rd. Calculating structures and free energies of complex molecules: combining molecular mechanics and continuum models. *Acc. Chem. Res.* **2000**, *33*, 889-897.

45. Tuccinardi, T.; Granchi, C.; Iegre, J.; Paterni, I.; Bertini, S.; Macchia, M.; Martinelli, A.; Qian, Y.; Chen, X.; Minutolo, F. Oxime-based inhibitors of glucose transporter 1 displaying antiproliferative effects in cancer cells. *Bioorg. Med. Chem. Lett.* **2013**, *23*, 6923-6927.
46. Tuccinardi, T.; Manetti, F.; Schenone, S.; Martinelli, A.; Botta, M. Construction and validation of a RET TK catalytic domain by homology modeling. *J. Chem. Inf. Model.* **2007**, *47*, 644-655.
47. Abdullaev, F.; Riveron-Negrete, L.; Caballero-Ortega, H.; Hernández, J. M.; Perez-Lopez, I.; Pereda-Miranda, R.; Espinosa-Aguirre, J. Use of in vitro assays to assess the potential antigenotoxic and cytotoxic effects of saffron (*Crocus sativus* L.). *Toxicol. in vitro* **2003**, *17*, 731-736.
48. Modaghegh, M. –H.; Shahabian, M.; Esmaeili, H. –A.; Rajbai, O.; Hosseinzadeh, H. Safety evaluation of saffron (*Crocus sativus*) tablets in healthy volunteers. *Phytomedicine* **2008**, *15*, 1032-1037.

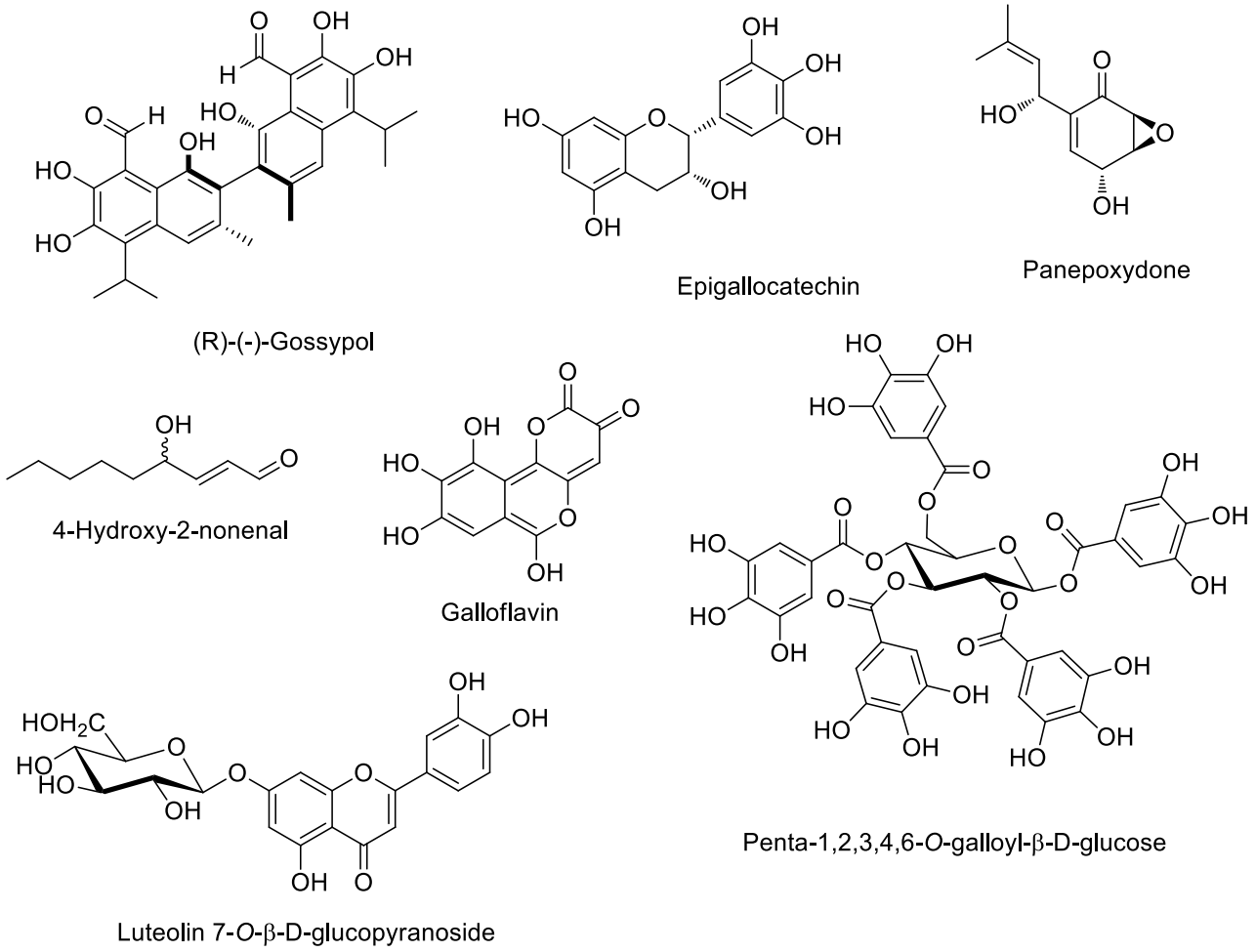
(R)-(-)-Gossypol
Epigallocatechin
Panepoxydone
4-Hydroxy-2-nonenal
Galloflavin
Penta-1,2,3,4,6-O-galloyl-β-D-glucose
Luteolin 7-O-β-D-glucopyranoside

Figure 1.

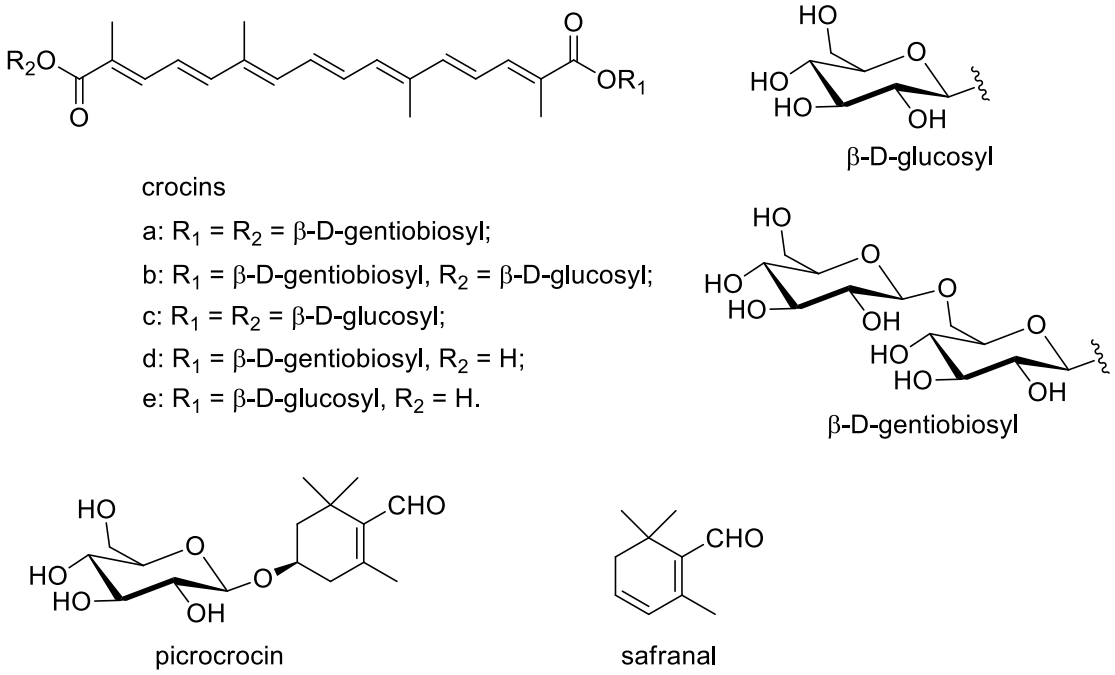
R2O
O
O
OR1
HO
O
HO
HO
OH
β-D-glucosyl
crocins
a: R1 = R2 = β-D-gentiobiosyl;
b: R1 = β-D-gentiobiosyl, R2 = β-D-glucosyl;
c: R1 = R2 = β-D-glucosyl;
d: R1 = β-D-gentiobiosyl, R2 = H;
e: R1 = β-D-glucosyl, R2 = H.
HO
O
HO
HO
OH
O
HO
HO
OH
O
β-D-gentiobiosyl
HO
O
HO
HO
OH
O
CHO
picrocrocin
CHO
safranal

Figure 2.

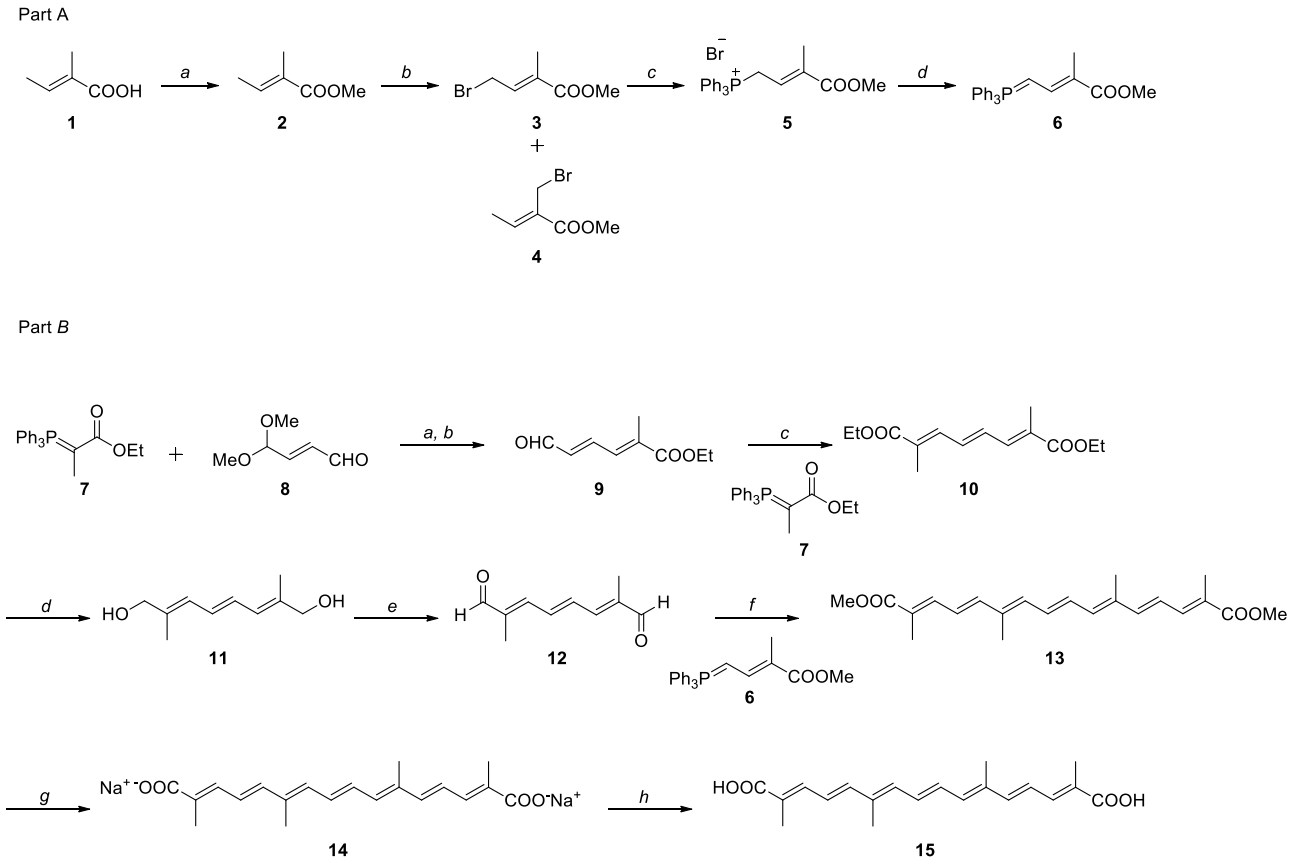
Part A
COOH
a
COOMe
b
Br
COOMe
c
Br⁻
Ph3P+
COOMe
d
Ph3P
COOMe
1
2
3
4
5
6
Part B
Ph3P
O
OEt
OMe
MeO
CHO
a, b
OHC
COOEt
c
EtOOC
COOEt
7
8
9
10
d
HO
OH
e
O
H
H
O
f
MeOOC
COOMe
11
12
13
6
g
Na+ -OOC
COO-Na+
h
HOOC
COOH
14
15

Scheme 1.

Table 1.

compound	*h*LDH-5	*h*LDH-1
	IC_{50}, μM	
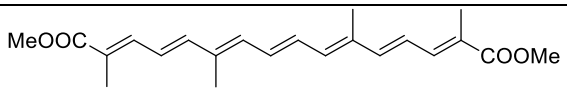 **13**	> 200	> 200
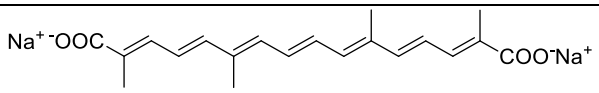 **14**	54.9 ± 4.7	> 200
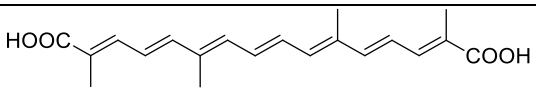 **15**	61.9 ± 2.3	> 200
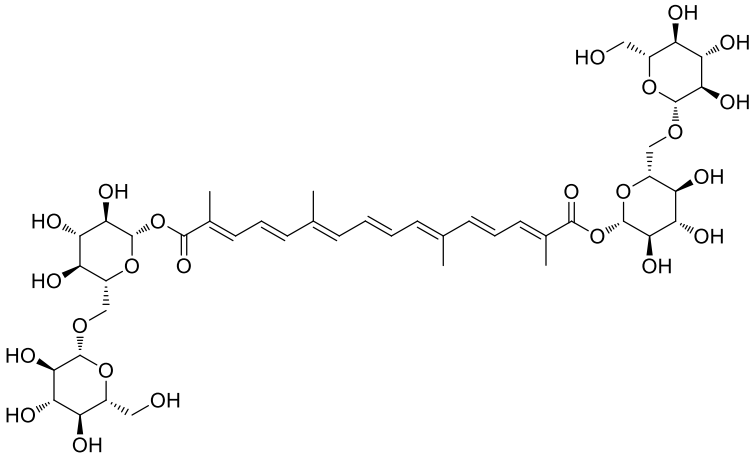 **16**	95.7 ± 9.8	59.8 ± 4.2
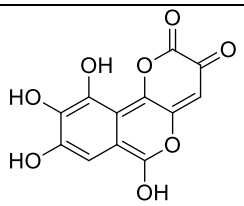 **Galloflavin**	93.2 ± 8.7	123.2 ± 14.2

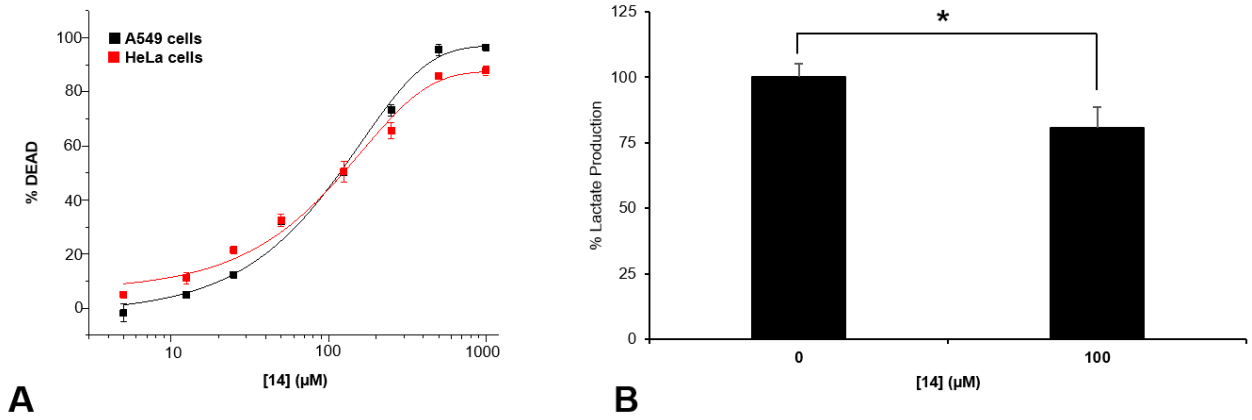
A549 cells
HeLa cells
% DEAD
[14] (μM)
A
% Lactate Production
*
0
100
[14] (μM)
B

Figure 3.

Table 2.

	EEL	VDW	ENPOLAR	EPB	ΔPBSA
Pose 1	-208.1	-29.8	-3.8	220.8	-20.9
Pose 2	-255.1	-36.3	-4.2	285.4	-10.2
Pose 3	-279.8	-28.6	-3.9	283.1	-29.2
Pose 4	-218.7	-24.7	-4.1	227.4	-20.1
Pose 5	-147.0	-22.5	-3.3	157.8	-15.0

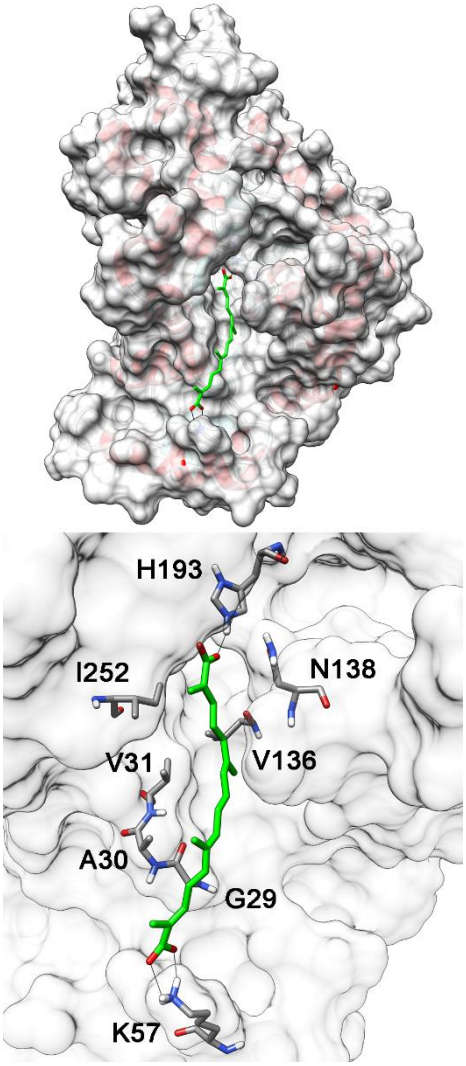

Figure 4.

Figure 1. Some representative naturally-derived compounds that inhibit *h*LDH-5.

Figure 2. Structures of saffron main metabolites.

Figure 3. Panel A: Dose-response curve for compound **14** in A549 and HeLa cells. Panel B: Lactate production inhibition for compound **14** in HeLa cells quantified by GC-MS. % DEAD is less than 28 % in all samples. Mean of three experiments. Error bars show SE (n=3). Statistical analysis was performed using an unpaired, two-tailed student's t test. * $p < 0.05$ relative to vehicle control.

Figure 4. Putative binding mode of compound **14** into *h*LDH-5. Putative binding pose of the ligand (green) in the binding site and view of the most relevant ligand–receptor interactions.

Scheme 1. *Reagents and conditions*. Part A: a) H_2SO_4, MeOH, reflux; b) NBS, BPO, $CHCl_3$, reflux; c) PPh_3, toluene, RT; recrystallization from CH_3CN/AcOEt; d) 0.5 M NaOH, DCM, RT. Part B: a) DCM, RT; b) Amberlyst 15, H_2O, acetone, RT; c) DCM, RT; d) DIBAL-H, an. hexane, -78 °C to -20 °C; e) activated MnO_2, acetone, 0 °C to RT; f) toluene, reflux; g) aq. NaOH, MeOH, reflux; h) H_3PO_4.

Table 1. Enzyme inhibition potencies.

Table 2. MM-PBSA results for the five different *h*LDH-5-compound 14 complexes. ΔPBSA is the sum of the electrostatic (EEL) and van der Waals (VDW), as well as polar (EPB) and non-polar (ENPOLAR) solvation free energy. Data are expressed as kcal/mol.

708

TABLE OF CONTENTS GRAPHICS